Electronic Supplementary Information

Synergistic Engineering of Dielectric and Magnetic Losses in M-Co/RGO Nanocomposites toward High-performance Microwave Absorption

Qi Li, [ab] Zheng Zhang, [ab] Xiaochen Xun, [ab] Fangfang Gao, [ab] Xuan Zhao, [ab] Zhuo Kang,[ab] Yi Ding,[c] Qingliang Liao,*[ab] and Yue Zhang *[ab]

[a.] Beijing Advanced Innovation Center for Materials Genome Engineering, Beijing Key Laboratory for Advanced Energy Materials and Technologies, University of Science and Technology Beijing, Beijing 100083, People's Republic of China. Email: liao@ustb.edu.cn, yuezhang@ustb.edu.cn

[b.] State Key Laboratory for Advanced Metals and Materials, School of Materials Science and Engineering, University of Science and Technology Beijing, Beijing 100083, People's Republic of China.

[c.] State Key Laboratory of Advanced Power Transmission Technology (Global Energy Interconnection Research Institute Co. Ltd.), Beijing 102209, China.

*** Corresponding author.**

Qingliang Liao, liao@ustb.edu.cn; Yue Zhang, yuezhang@ustb.edu.cn

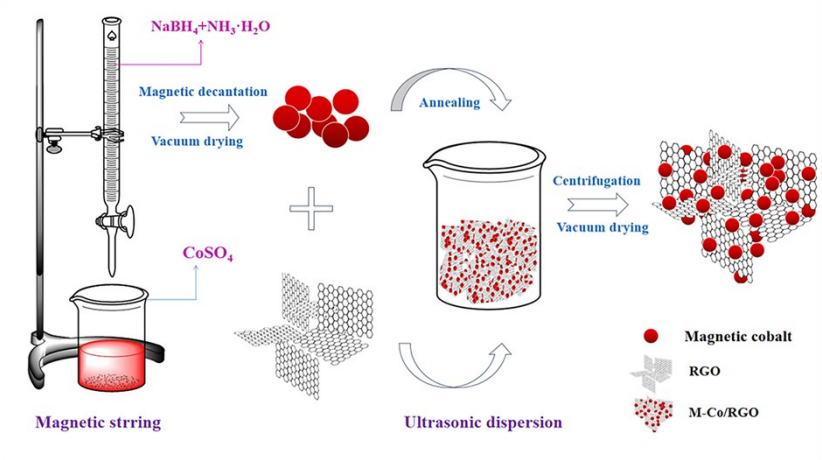

Fig. S1. Schematic illustration of the formation process for M-Co/RGO nanocomposites.

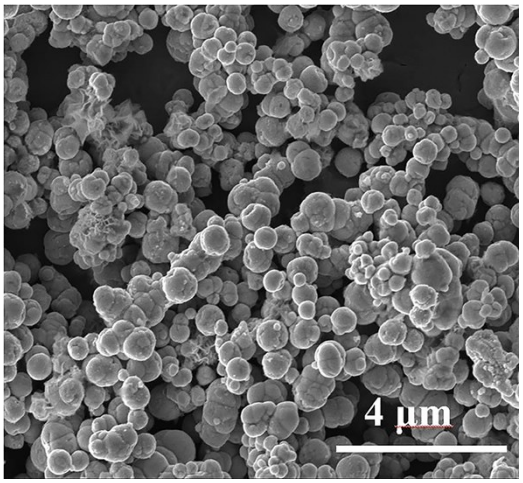

Fig. S2. SEM image of M-Co nanoparticles.

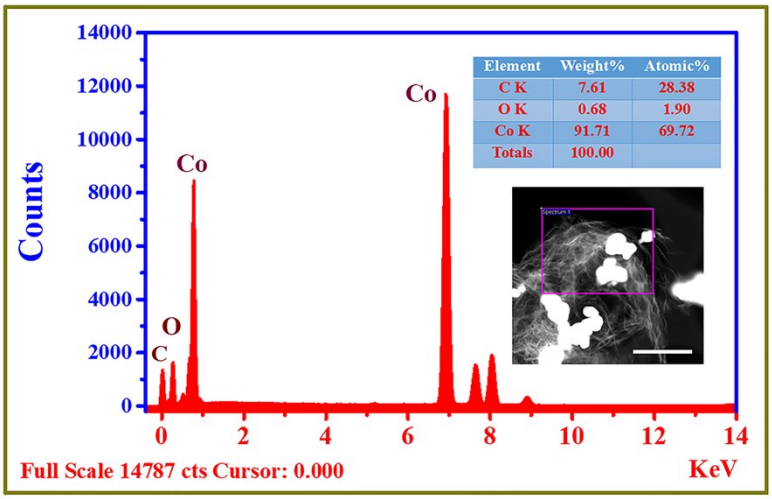

Fig. S3. EDS spectra of M-Co/RGO nanocomposites

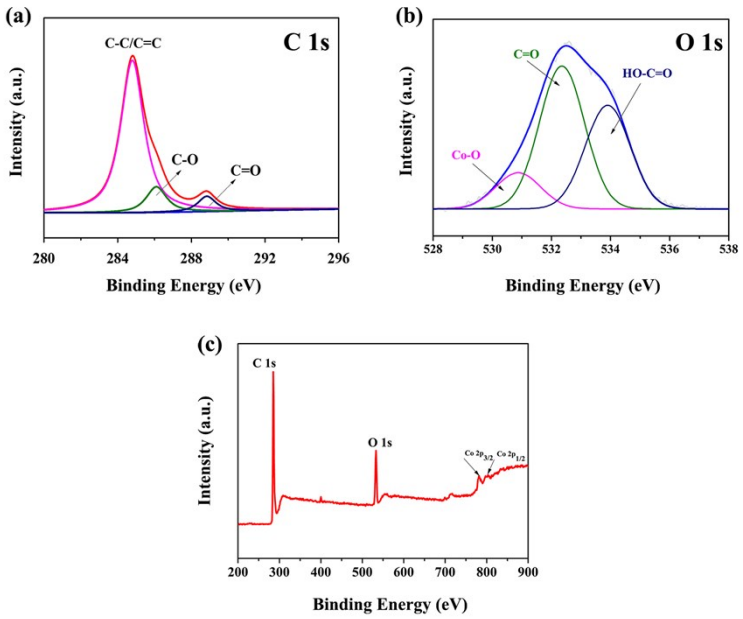

Fig. S4. (a) C 1s XPS spectra for M-Co/RGO nanocomposites. (b) O 1s XPS spectra for M-Co/RGO nanocomposites. (c) XPS spectra of the M-Co/RGO nanocomposites.

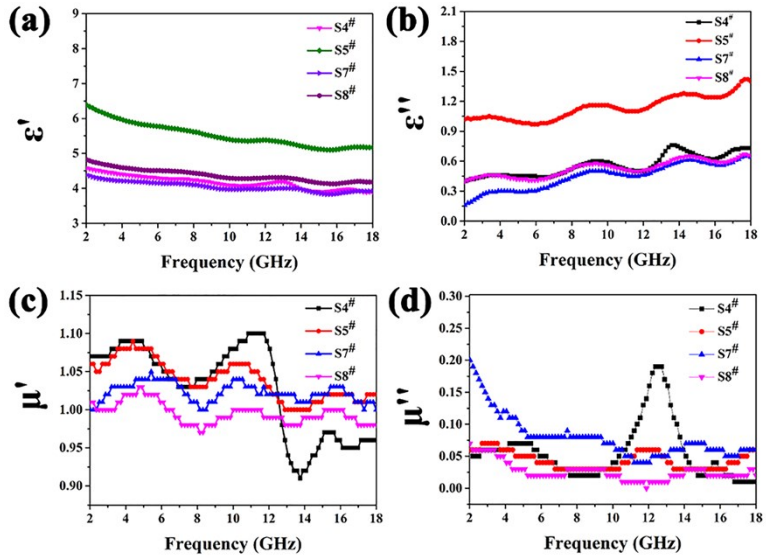

Fig. S5. EM parameters of the S4#, S5#, S7# and S8# in the frequency range of 2-18 GHz: (a) ε', (b) μ', (c) ε'', (d) μ''.

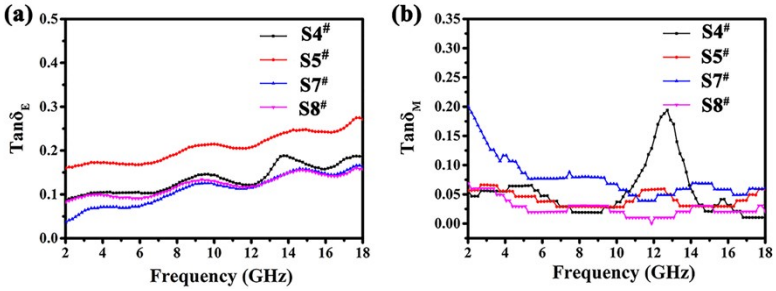

Fig. S6. (a) $\tan\delta_E$ and (b) $\tan\delta_M$ of S4#, S5#, S7# and S8# in the frequency range of 2-18 GH

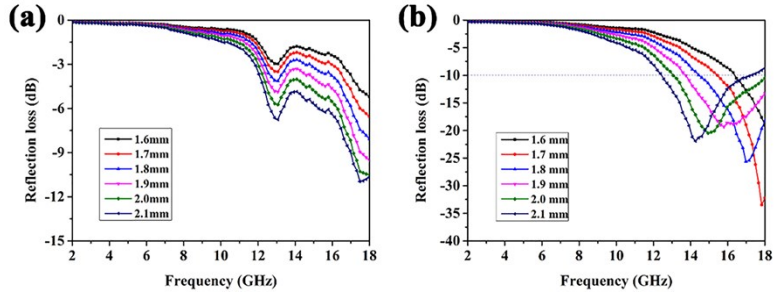

Fig. S7. RL curves of M-Co/RGO nanocomposites with different thicknesses in the frequency range 2-18 GHz: (a) S1#, (b) S2#.

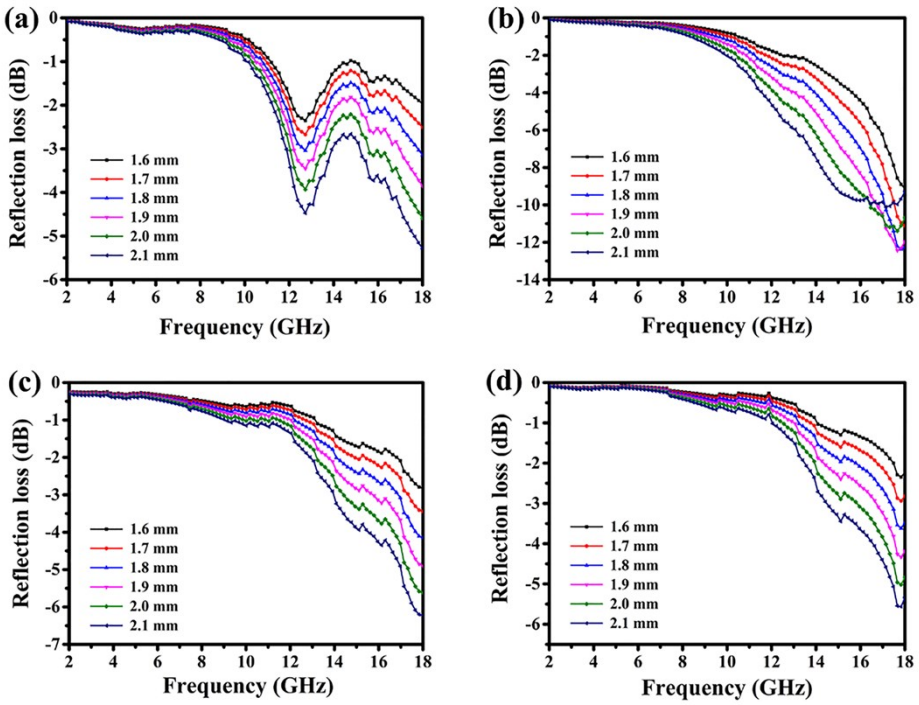

Fig. S8. RL curves of M-Co/RGO nanocomposites with different thicknesses in the frequency range 2-18 GHz: (a) S4#, (b) S5#, (c) S7#, (d) S8#.

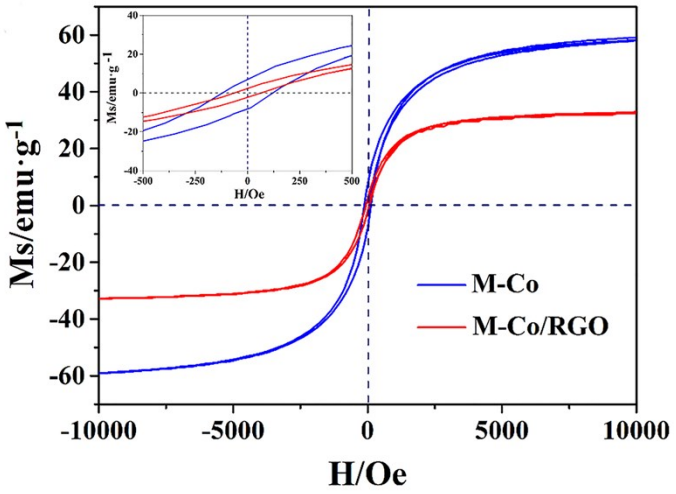

Fig. S9. Magnetic hysteresis loop of M-Co nanoparticles and M-Co/RGO nanocomposites (S3#) at 300 K (the inset is amplified views of hysteresis loops at low applied fields).

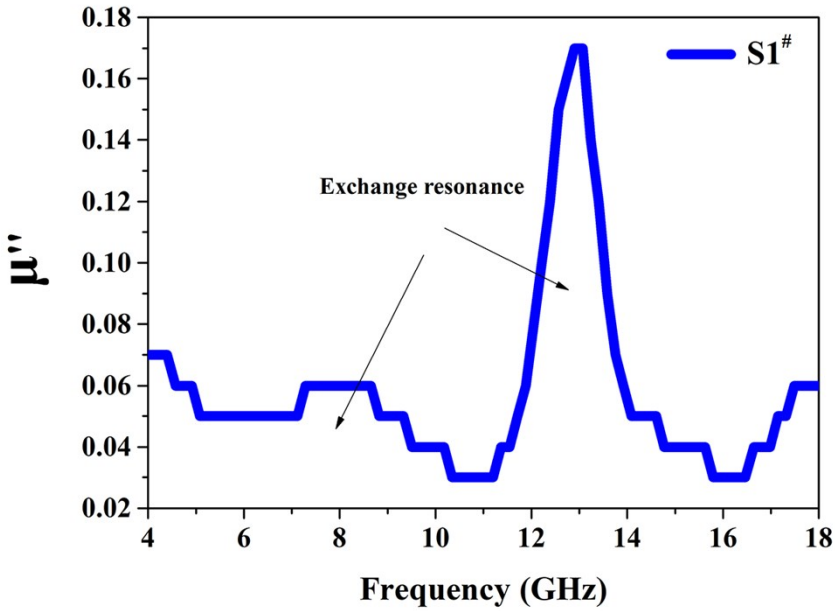

Fig. S10. Frequency dependence of μ" for S1# in the frequency range of 4-18 GHz.

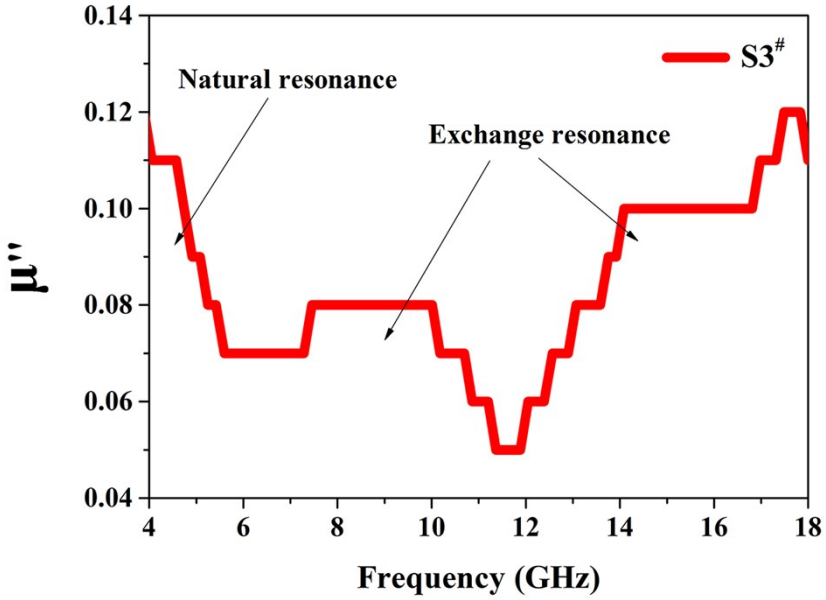

Fig. S11. Frequency dependence of μfor S3# in the frequency range of 4-18 GHz.

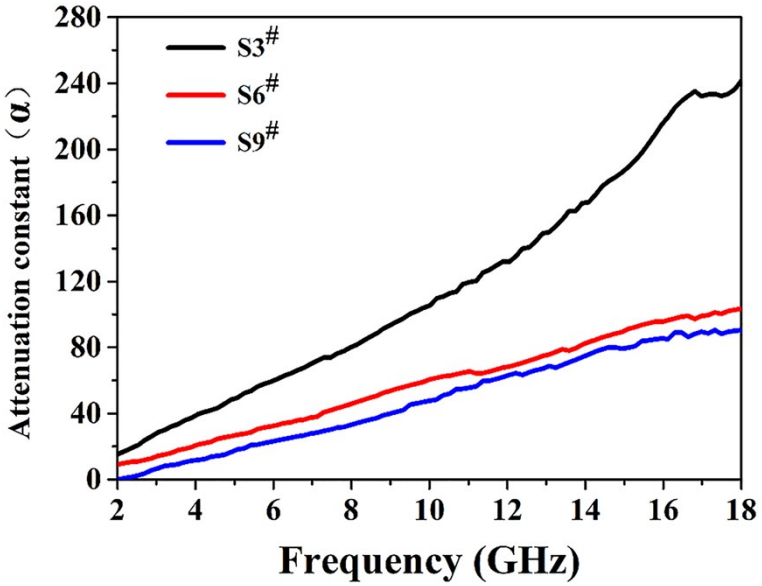

Fig. S12.Attenuation constant α of S3#, S6# and S9#.

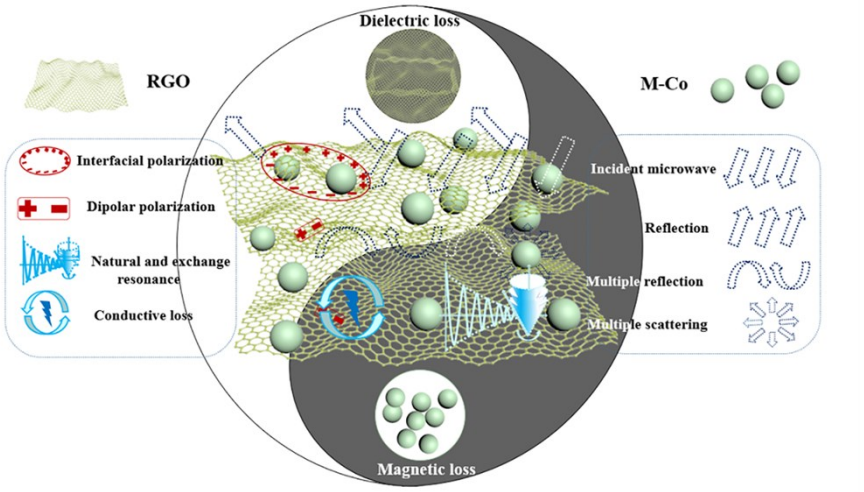

Fig. S13. Schematic illustration of microwave absorption mechanism of M-Co/RGO nanocomposites

Supporting Information table

Table S1. The different mass ratio and filler loading of M-Co/RGO nanocomposites.

Sample	S1#	S2#	S3#	S4#	S5#	S6#	S7#	S8#	S9#
M-Co:RGO	5:1	5:1	5:1	10:1	10:1	10:1	15:1	15:1	15:1
Filler loading	10%	15%	20%	10%	15%	20%	10%	15%	20%